## Possible routes for synthesis of new boron-rich Fe-B and $Fe_{1-x}Cr_xB_4$ compounds

A.F. Bialon, T. Hammerschmidt, R. Drautz, S. Shah, E.R. Margine, and A.N. Kolmogorov Atomistic Modelling and Simulation, ICAMS, Ruhr-Universität Bochum, D-44801 Bochum, Germany and Department of Materials, University of Oxford, Parks Road, Oxford OX1 3PH, United Kingdom (Dated: November 30, 2018)

We use ab initio calculations to examine thermodynamic factors that could promote the formation of recently proposed unique oP10-FeB<sub>4</sub> and oP12-FeB<sub>2</sub> compounds. We demonstrate that these compact boron-rich phases are stabilized further under pressure. We also show that chromium tetraboride is more stable in the new oP10 rather than the reported oI10 structure which opens up the possibility of realizing an oP10-(Fe<sub>x</sub>Cr<sub>1-x</sub>)B<sub>4</sub> pseudobinary material. In addition to exhibiting remarkable electronic features, oP10-FeB<sub>4</sub> and oP12-FeB<sub>2</sub> are expected to be harder than the known Fe-B compounds commonly used for hard coating applications.

The renewed interest in transition metal (TM) borides stems, in part, from the materials' potential to serve as hard, wear-resistant, chemically inert coatings.<sup>1–5</sup> Combination of the TM and boron ensures a high valence electron density and a pronounced covalent bonding resulting in the compounds' exceptional hardness; for example, ReB<sub>2</sub> has been recently demonstrated to be the first metal-based bulk material that can scratch diamond.<sup>1,5</sup> Metallicity and covalency are also key ingredients for phonon-mediated superconductivity and TM borides have received a lot of attention<sup>6</sup> following the discovery of a remarkable MgB<sub>2</sub> superconductor.<sup>7</sup>

Iron borides have two particularly important industrial applications. First, homogeneously dispersed secondphase particles of Fe<sub>2</sub>B are known to improve the tensile strength of low-carbon steels<sup>8</sup> while pseudobinary  $Fe_3(B,C)$  and  $Fe_{23}(B,C)_6{}^{9,10}$  precipitates harden highcarbon steels. 11 Second, Fe-B-based hard protective coatings are produced directly on the surface of steel via the process of boriding. 12–14 During this thermochemical process boron diffuses into the steel forming either a single-phase (Fe<sub>2</sub>B) or a duplex-phase (Fe<sub>2</sub>B+FeB) coating layer. 13 The two FeB and Fe<sub>2</sub>B compounds have been shown to crystallize in the oP8 (or the related oS8)<sup>15</sup> and tI12 configurations, respectively, and are the only low-temperature ground states listed in the latest experimental phase diagram. <sup>16</sup> Synthesis of new boron-rich Fe-B compounds could have technological implications as the hardness of metal borides tends to increase with boron content. So far, except for the observation of a metastable FeB<sub>49</sub> intercalation compound<sup>17</sup> only two studies reported on the synthesis of amorphous<sup>18</sup> and the AlB<sub>2</sub>-type<sup>19</sup> iron diboride but these compounds have not been reproduced.

Application of advanced compound prediction methods has recently allowed us to identify oP12-FeB<sub>2</sub> and oP10-FeB<sub>4</sub> candidate ground states with unique crystal structures (Fig. 1b,c) that are stable relative to the known compounds. <sup>20</sup> oP12-FeB<sub>2</sub> was predicted to be the first metal diboride semiconductor while oP10-FeB<sub>4</sub> was shown to have the necessary features to exhibit phonon-mediated superconductivity with a  $T_c$  of 15-20 K. The aim of this study is to examine synthesis routes that could lead to the discovery of the new materials. We

find that both compounds are stabilized further under pressure while the oP10 Fe-based phase could be realized in the  $(Fe_xCr_{1-x})B_4$  pseudobinary form. We also observe that calculated elastic constants of the predicted Fe-B compounds are higher than those in the known FeB and Fe<sub>2</sub>B materials.

We use the projector augmented wave method<sup>21</sup> as implemented in VASP<sup>22</sup> and carry out full structural and spin relaxation for all compounds; relevant  $MB_2$  and MB<sub>4</sub> metal borides show no magnetic ordering and their phonon and electron-phonon (e-ph) properties are examined without spin polarization. The chosen energy cutoff of 500 eV and dense Monkhorst-Pack k-meshes<sup>23</sup> ensure numerical convergence of formation energy differences to typically 1-2 meV/atom. We employ the Perdew-Burke-Ernzerhof (PBE) exchange-correlation (xc) functional<sup>24</sup> within the generalized gradient approximation (GGA). Vibrational corrections to Gibbs energy are calculated with PHON. 25 The strength of the e-ph coupling for oP10-CrB<sub>4</sub> is evaluated within the linear response theory using the Quantum-ESPRESSO package. 26 The boron ground state is simulated as  $\alpha$ -B, known to be stable at medium pressures up to  $\sim$  19 GPa. 27,28 The iron ground state is taken as bcc and hcp at 0 and 20 GPa,  ${\it respectively.}^{29}$ 

The peculiar oI10-TMB<sub>4</sub> phases comprised of tetragonal B nets (Fig. 1a) were previously examined within the extended Hückel method; it was concluded that maximum binding in the 3d series is achieved for Cr and that the electron-rich Fe, Co, and Ni tetraborides may be unstable in this configuration.<sup>30</sup> Our calculations showed<sup>20</sup> dynamical instability of the oI10-FeB<sub>4</sub> phase which gains a considerable 0.13 eV/f.u. in enthalpy by transforming into the oP10 structure (Fig. 2b). In the present study we observe a similar behaviour in the Cr-B system: oI10-CrB<sub>4</sub> is found to be both dynamically (Fig. 1 in Ref. 31) and thermodynamically (by 0.03 eV/f.u.) unstable relative to oP10. Although the boron network undergoes a significant distortion in the oI10→oP10 transformation, the lattice parameters and the simulated powder diffraction patterns (Fig. 2 in Ref. 31) remain close which may explain why the structure of CrB<sub>4</sub> was originally solved as oI10. These findings suggest that  $Fe_xCr_{1-x}B_4$ compositions may assume the oP10 structure as well un-

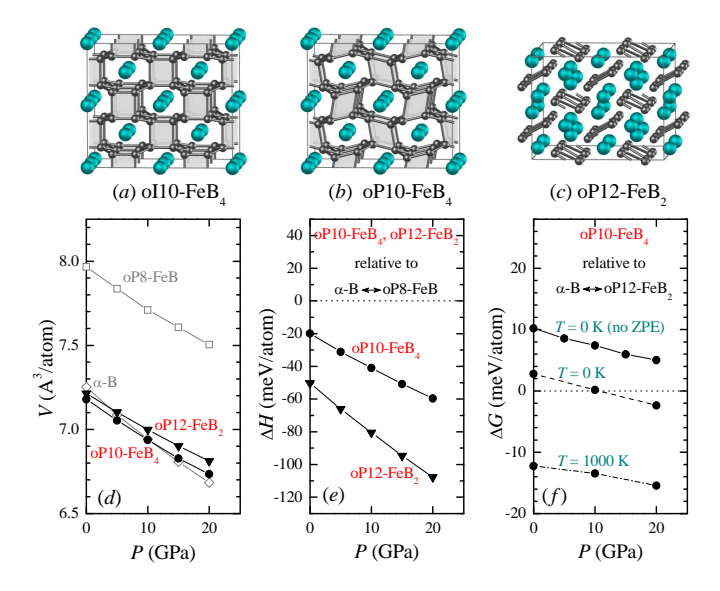


FIG. 1: (Color online) a–c) Boron-rich structures: iron and boron are shown as large cyan and small black spheres, respectively. d) Atomic volume as a function of pressure. e) Relative enthalpy of oP12-FeB<sub>2</sub> and oP10-FeB<sub>4</sub> candidate phases w.r.t. the  $\alpha$ -B $\leftrightarrow$ oP8-FeB tie-line. f) Relative Gibbs energy (with vibrational contributions included using PHON<sup>25</sup>) of oP10-FeB<sub>4</sub> w.r.t.  $\alpha$ -B $\leftrightarrow$ oP12-FeB<sub>2</sub> at 0 K with and without zero point energy (ZPE) and at 1000 K.

der standard synthesis conditions. Indeed, there were no special requirements regarding the heat treatment or the starting materials (apart from cold compacting of the MB powders<sup>32,33</sup>) for the past synthesis of ternary Fe-Cr-B materials, e.g., the ordered metal-rich Mn<sub>4</sub>B-type alloy<sup>34</sup> or the oP8-FeB- and oS8-CrB-type compounds with partial substitutions of the host metal.<sup>32,33</sup>

The effect of the composition on the thermodynamic and electronic properties of the ordered oP10- $Fe_xCr_{1-x}B_4$  compounds is investigated via supercell simulations,<sup>35</sup> see Fig. 2. We observe a sizeable stabilization, up to 28 meV/f.u., of the oP10 structure at x = 0.5, Fig. 2a. The configurational entropy contribution from the disorder in population of metal sites is comparable at elevated temperatures:  $\Delta G_{conf}(T) =$  $-k_BT[x\ln x + (1-x)\ln(1-x)]$  would be 60 meV/f.u. at T=1000 K and x=0.5 if all decorations were degeneratein energy. Hence, the resulting ordering of Fe and Cr on the metal sublattice will depend on the quenching conditions. The density of states (DOS) is found to be sensitive to metal site population patterns at the Fe-rich end and drops rapidly in going from pure FeB<sub>4</sub> (1.0 states/(spin eV atom)) to pure CrB<sub>4</sub> (0.18 states/(spin eV atom)), Fig. 2b. Our linear response theory calculations<sup>26,36</sup> give a small e-ph coupling ( $\lambda \approx 0.15$ ) and a negligible critical temperature  $(T_c \ll 1 \text{ K})$  in oP10-CrB<sub>4</sub> indicating that superconductivity in this pseudobinary will require high Fe concentrations.

Application of medium pressures (a few GPa) in multi-

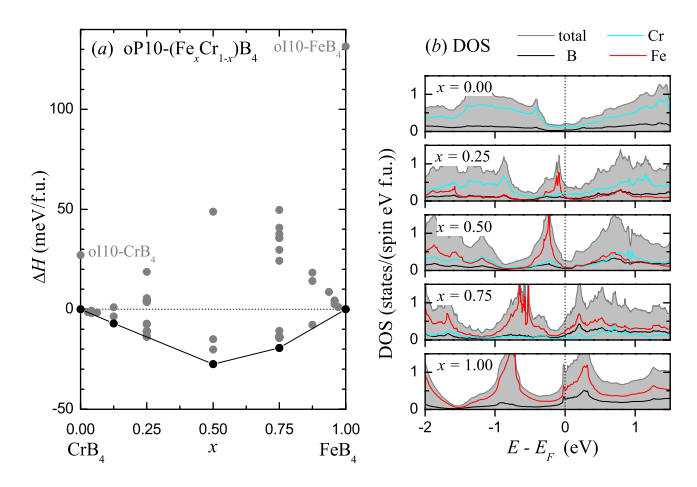


FIG. 2: (Color online) a) Relative stability of the pseudobinary oP10-Fe<sub>x</sub>Cr<sub>1-x</sub>B<sub>4</sub> compound. b) Total and projected density of states (DOS) for lowest enthalpy compounds.

anvil or diamond anvil cell setups may promote the formation of the materials in the predicted configurations by improving the compounds' thermodynamic stability or the reaction kinetics. Successful examples of this synthesis route include boron-rich CaB<sub>4</sub> and NdB<sub>6</sub> or metal-rich Fe<sub>2</sub>B materials.<sup>37–39</sup> We have examined the response to the hydrostatic pressure of over 40 known and proposed ambient-pressure M-B structure types listed in Ref. 31 by calculating their formation enthalpies at P = 20 GPa. We find that oP8-FeB is the lowest-enthalpy phase and that the necessary condition for a boron-rich phase to be thermodynamically stable is to lie below the oP8-FeB $\leftrightarrow \alpha$ -B tie-line. Due to the remarkable compactness (Fig. 1d) of the predicted oP10-FeB<sub>4</sub> and oP12-FeB<sub>2</sub> phases (a respective 5% and 7% reduction in atomic volume compared to mixture of  $\alpha$ -B and FeB) pressure does lead to much lower relative formation enthalpies for both compounds (Fig. 1e). Above P = 10 GPa, oP10-FeB<sub>4</sub> becomes thermodynamically stable relative to  $\alpha$ -B and oP12-FeB<sub>2</sub> at all temperatures (Fig. 1f).

The compactness of these Fe-B phases also opens the perspective of obtaining new metal-based hard materials. It has been argued that the extraordinary hardness

	$\mathrm{Fe_{2}B}$		FeB		$\mathrm{FeB}_2$	FeB <sub>4</sub>	${\rm ReB_2}$
	tI12	oP8	oS8	tI16	oP12	oP10	hP6
B(GPa)	228	287	257	286	311	274	339
G(GPa)	143	138	153	157	231	187	266
E(GPa)	355	358	383	399	556	457	632
$\nu$	0.24	0.29	0.25	0.27	0.20	0.22	0.19

TABLE I: Calculated bulk (B), shear (G), and Young (E) moduli and Poisson ratio  $(\nu)$  for known and predicted Fe-B phases. hP6-ReB<sub>2</sub> is added for comparison.

of the ReB<sub>2</sub> material arises from an efficient packing of B into hcp-Re that results in only a 5% expansion of the metal lattice and, consequently, in the shortest TM-TM distances for any TM diboride. The importance of having strong TM-TM and TM-B bonds is that the (0001) plane in hP6-ReB<sub>2</sub> supports the weakest stress. In the predicted oP12-FeB<sub>2</sub>, the TM-TM (TM-B) bonds are shorter by 11% (9%) not only because of the smaller size of Fe but also because of the break-up of the B lavers into B chains which tilt to accommodate the metal atoms (Fig. 3 in Ref. 31). This leads to a more pronounced relative deviation from Vegard's law<sup>40</sup> in oP12- $FeB_2$  (-16.4%) compared to that in hP6-ReB<sub>2</sub> (-6.4%). A qualitative analysis of the materials hardness can be done by comparing shear moduli, as they have been shown to correlate with hardness in some cases.<sup>2</sup> The shear moduli in the predicted B-rich phases are at least as high as in the known oP8-FeB and tI12-Fe<sub>2</sub>B compounds (Table I). Although elastic constants alone are not sufficient for a quantitative prediction of materials hardness, 41 it is encouraging to find the elastic moduli and the Poisson ratio in oP12-FeB<sub>2</sub> to be comparable to those in hP6ReB<sub>2</sub> (see Tables I and II in Ref. 31 for comparison of experimental and theoretical values).

In summary, our high-throughput simulations spanning a large library of known and proposed structures predict consistently that new compounds should form under accessible synthesis conditions in such a common binary system as Fe-B. Ground state search under ambient or elevated pressures can be expanded further by performing unrestricted structural optimization driven, e.g., by evolutionary algorithms<sup>20</sup> for larger unit cells and other Fe-B compositions. Due to the known exceptional complexity of metal boride structures<sup>42</sup> experimental input may be key for determination of the true ground states

ANK and SS acknowledge the support of the EP-SRC. AFB, TH and RD acknowledge financial support through ThyssenKrupp AG, Bayer MaterialScience AG, Salzgitter Mannesmann Forschung GmbH, Robert Bosch GmbH, Benteler Stahl/Rohr GmbH, Bayer Technology Services GmbH and the state of North-Rhine Westphalia as well as the EU in the framework of the ERDF.

- <sup>1</sup> H.-Y. Chung, M. B. Weinberger, J. B. Levine, A. Kavner, J.-M. Yang, S. H. Tolbert, and R. B. Kaner, Science 316, 436 (2007).
- <sup>2</sup> H.-Y. Chung, M.B. Weinberger, J.-M. Yang, S.H. Tolbert, and R.B. Kaner, Appl. Phys. Lett. **92**, 261904 (2008).
- <sup>3</sup> Q. Gu, G. Krauss, and W. Steurer, Adv. Mater. **20**, 3620 (2008).
- <sup>4</sup> M.B. Weinberger, J.B. Levine, H.-Y. Chung, R.W. Cumberland, H.I. Rasool, J.-M. Yang, R.B. Kaner, and S.H. Tolbert, Chem. Mater. 21, 1915 (2009).
- <sup>5</sup> J.B. Levine, S.H. Tolbert, and R.B. Kaner, Adv. Funct. Mater. **19**, 3519 (2009).
- <sup>6</sup> J.W. Simonson, D. Wu, S.J. Poon, and S.A. Wolf, J. Supercond. Nov. Magn. 23, 417 (2010) and references therein.
- J. Nagamatsu, N. Nakagawa, T. Muranaka, Y. Zenitani, and J. Akimitsu, Nature (London) 410, 63 (2001).
- <sup>8</sup> J.A. Jiménez, G. González-Doncel and O.A. Ruano, Adv. Mater. 7, 130 (1995).
- <sup>9</sup> L. Lanier, G. Metauer and M. Moukassi, Mikrochim. Acta 114/115, 353 (1994).
- <sup>10</sup> S. Watanabe and H. Ohtani, Transactions ISIJ 23, 38 (1983).
- <sup>11</sup> S. Watanabe, H. Ohtani and T. Kunitake, Transactions ISIJ 23, 120 (1983).
- <sup>12</sup> I. Campos, J. Oseguera, U. Figueroa, J.A. García, O. Bautista, and G. Kelemenis, Mater. Sci. Eng. A352, 261 (2003).
- <sup>13</sup> S. Sen, U. Sen, and C. Bindal, Vacuum **77**, 195 (2005).
- O. Culha, M. Toparli, and T. Aksoy, Adv. Eng. Softw. 40, 1140 (2009).
- V.A. Barinov, G.A. Dorofeev, L.V. Ovechkin, E.P. Elsukov and A.E. Ermakov, Phys. Stat. Sol. A **123**, 527 (1991);
  T. Kanaizuka, Phys. Stat. Sol. A **69**, 739 (1982).
- <sup>16</sup> T. van Rompaey, K.C. Hari Kumar, and P. Wollants, J. Alloys Compd. 334, 17 3 (2002).

- <sup>17</sup> K. Balani, A. Agarwala, and N.B. Dahotre, J. Appl. Phys. 99, 044904 (2006).
- <sup>18</sup> K. Moorjani, T.O. Poehler, F.G. Satkiewicz, M.A. Manheimer, D.J. Webb and S.M. Bhagat, J. Appl. Phys 57, 3445 (1985)
- <sup>19</sup> L.G. Voroshnin, L.S. Lyakhovich, G.G. Panich, and G.F. Protasevich, Met. Sci. Heat Treat. [Metal. i Term. Obrabotka Metal.] 9, 732 (1970).
- <sup>20</sup> A.N. Kolmogorov, S. Shah, E.R. Margine, A.F. Bialon, T. Hammerschmidt, and R. Drautz, Phys. Rev. Lett. **105**, 217003 (2010).
- <sup>21</sup> P. E. Blöchl, Phys. Rev. B **50**, 17953 (1994).
- <sup>22</sup> G. Kresse and J. Hafner, Phys. Rev. B 47, 558 (1993); G. Kresse and J. Furthmüller, Phys. Rev. B 54, 11169 (1996).
- <sup>23</sup> J. D. Pack and H. J. Monkhorst, Phys. Rev. B **13**, 5188 (1976); **16**, 1748 (1977).
- <sup>24</sup> J.P. Perdew, K. Burke, and M. Ernzerhof, Phys. Rev. Lett. 77, 3865 (1996).
- <sup>25</sup> D. Alfè, Comp. Phys. Commun. **180**, 2622 (2009).
- P. Giannozzi, S. Baroni, N. Bonini, M. Calandra, R. Car, C. Cavazzoni, D. Ceresoli, G.L. Chiarotti, M. Cococcioni, I. Dabo, A. Dal Corso, S. de Gironcoli, S. Fabris, G. Fratesi, R. Gebauer, U. Gerstmann, C. Gougoussis, A. Kokalj, M. Lazzeri, L. Martin-Samos, N. Marzari, F. Mauri, R. Mazzarello, S. Paolini, A. Pasquarello, L. Paulatto, C. Sbraccia, S. Scandolo, G. Sclauzero, A.P. Seitsonen, A. Smogunov, P. Umari, and R.M. Wentzcovitch, J. Phys.: Condens. Matter 21, 395502 (2009).
- <sup>27</sup> M.J. van Setten, M.A. Uijttewaal, G.A. de Wijs, and R.A. de Groot, J. Am. Chem. Soc. **129**, 2458 (2007).
- <sup>28</sup> A.R. Oganov, J.H. Chen, C. Gatti, Y.Z. Ma, Y.M. Ma, C.W. Glass, Z.X. Liu, T. Yu, O.O. Kurakevych, and V.L. Solozhenko, Nature (London) 457, 863 (2009).
- <sup>29</sup> M. Ekman, B. Sadigh, K. Einarsdotter, and P. Blaha, Phys. Rev. B **58**, 5296 (1998).

- <sup>30</sup> J.K. Burdett and E. Canadell, Inorg. Chem. **27**, 4437 (1988).
- <sup>31</sup> See supplementary material at [URL will be inserted by AIP] for additional explanations, figures and tables.
- <sup>32</sup> M. Carbucicchio, C. Grazzi, G. Palombarini, M. Rateo, and G. Sambogna, Hyp. Interact. 139/140, 393 (2002).
- <sup>33</sup> M. Carbucicchio, G. Palombarini, M. Rateo, and G. Sambogna, Hyp. Interact. 116, 143 (1998).
- <sup>34</sup> D.J. Beerntsen, Acta Cryst. **17**, 448 (1962).
- $^{35}$  Since  $W_{0.5}Os_{0.5}B_2$  is known to assume the  $ReB_2$  prototype  $^3$  we also examined ordered  $Fe_{0.5}Cr_{0.5}B_4$  in the related  $mS10\text{-}MnB_4$  supercell configurations but found them to be less stable by 22~meV/f.u w.r.t. the  $CrB_4\text{-}FeB_4$  tie-line.
- We employ ultrasoft pseudopotentials [D. Vanderbilt, Phys. Rev. B **41**, R7892 (1990)] with a cutoff of 43 and 344 Ry for the wave functions and charge density, respectively. A  $6\times6\times12$  k-point mesh with a Gaussian smearing of 0.02

- Ry and a  $3\times3\times6$  q-mesh are used for phonon dispersion calculations; a  $12\times12\times24$  k-mesh is used to evaluate the e-ph coupling. Calculation of the electron-phonon coupling in oP10-FeB<sub>4</sub> with these settings gives  $\lambda\approx0.8$ .
- <sup>37</sup> Z. Liu, X. Han, D. Yu, Y. Sun, B. Xu, X.F. Zhou, J. He, H.T. Wang, and Y. Tian, Appl. Phys. Lett. **96**, 031903 (2010).
- <sup>38</sup> X. Zhao, X. Liu, F. Lin, W. Liu, and W. Su, J. Alloys Comp. **249**, 247 (1997).
- <sup>39</sup> B. Yao, W.H. Su, F.S. Li, B.Z. Ding, and Z.Q. Hu, J. Mat. Sci. Lett. **16**, 1991 (1997).
- <sup>40</sup> The relative deviation is defined as  $V_{\rm MB_2}/(2/3V_{\rm B}+1/3V_M)-1$ ; all volumes are per atom.
- <sup>41</sup> P. Lazar and R. Podloucky, Phys. Rev. B **78**, 104114 (2008)
- <sup>42</sup> A.N. Kolmogorov and S. Curtarolo, Phys. Rev. B **74**, 224507 (2006) and references therin.

## Supplementary material to: Possible routes for synthesis of new boron-rich Fe-B and $Fe_{1-x}Cr_xB_4$ compounds

A.F. Bialon, <sup>1</sup> T. Hammerschmidt, <sup>1</sup> R. Drautz, <sup>1</sup> S. Shah, <sup>2</sup>, E.R. Margine, <sup>2</sup> and A.N. Kolmogorov <sup>2</sup> Atomistic Modelling and Simulation, ICAMS, Ruhr-Universität Bochum, D-44801 Bochum, Germany and <sup>2</sup> Department of Materials, University of Oxford, Parks Road, Oxford OX1 3PH, United Kingdom (Dated: November 30, 2018)

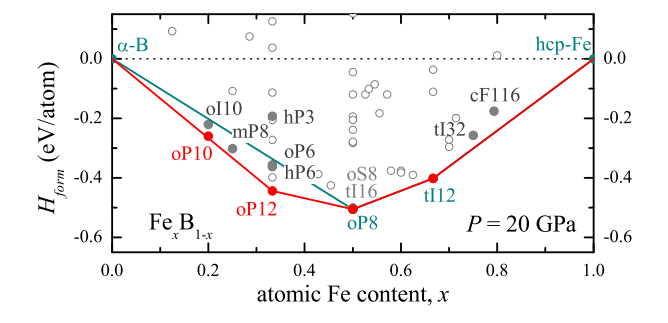


FIG. 1: (Color online) Calculated formation enthalphy of Fe-B compounds at P=20 GPa. The cyan and red labels correspond to known and proposed ground states, respectively.

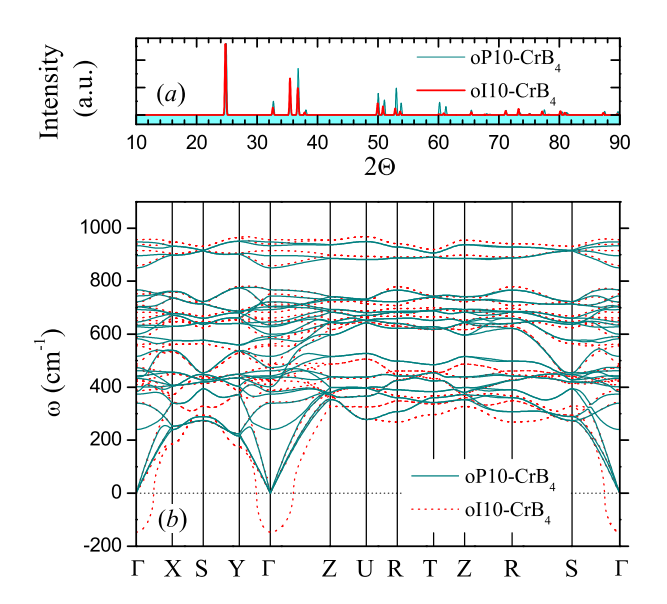


FIG. 2: (Color online) Comparison of competing oI10- and oP10-CrB<sub>4</sub> structures with relaxed lattice vectors of a=4.749 Å, b=5.488 Å, c=2.852 Å and a=4.723 Å, b=5.474 Å, c=2.851 Å, respectively: a) simulated x-ray patterns for  $\lambda=1.5418$  Å; b) calculated phonon dispersons showing dynamic instability of oI10-CrB<sub>4</sub> at  $q=\Gamma$ .

Library of structure types. We have considered over 40 commonly seen M-B and M-C structure types listed in the Inorganic Crystal Structure Database (ICSD).<sup>1</sup> The list below is ordered by composition and specifies the Pearson symbol and the prototype for each entry.

1:12: cF52-UB<sub>12</sub>; 1:7: oI64-MgB<sub>7</sub>; 3:20: oS46-Na<sub>3</sub>B<sub>20</sub>; 1:6: cP7-CaB<sub>6</sub>; 3:14: tI160-Li<sub>3</sub>B<sub>14</sub>; 1:4: tP20-UB<sub>4</sub>, oI10-CrB<sub>4</sub>, mS10-MnB<sub>4</sub>; 1:3: tP20-LiB<sub>3</sub>, hP16-Mo<sub>0.8</sub>B<sub>3</sub>; 2:5: hR21-Mo<sub>2</sub>B<sub>4.65</sub>; 1:2: hP3-AlB<sub>2</sub>, oP6-RuB<sub>2</sub>, hR18-MoB<sub>2</sub>, oP12-PbCl<sub>2</sub>, hP6-ReB<sub>2</sub>, hP6-MoS<sub>2</sub>; 2:3: oS20-V<sub>2</sub>B<sub>3</sub>, hP10-Ru<sub>2</sub>B<sub>3</sub>; 3:4: oI14-Ta<sub>3</sub>B<sub>4</sub>; 5:6: oS22-V<sub>5</sub>B<sub>6</sub>; 1:1: oP8-FeB-b, oS8-PtB<sub>0.67</sub>, tI16-MoB, oS8-TII, oP8-TiSi, hP2-WC; 5:4: hP18-Rh<sub>5</sub>B<sub>4</sub>; 11:8: oP38-Ru<sub>11</sub>B<sub>8</sub>; 3:2: tP10-U<sub>3</sub>Si<sub>2</sub>, aP30-Rh<sub>9</sub>B<sub>5.5</sub>; 5:3: tI32-Cr<sub>5</sub>B<sub>3</sub>; 2:1: tI12-CuAl<sub>2</sub>; 7:3: hP20-Th<sub>7</sub>Fe<sub>3</sub>, oP40-Mn<sub>7</sub>C<sub>3</sub>; 5:2: mS28-Mn<sub>5</sub>C<sub>2</sub>; 3:1: oP16-Fe<sub>3</sub>C, oS16-Re<sub>3</sub>B, tI32-Ni<sub>3</sub>P; 23:6: cF116-Cr<sub>23</sub>C<sub>6</sub>; 4:1: tP10-Be<sub>4</sub>B. The structures proposed in our previous study<sup>2</sup> include 1:4: oP10-FeB<sub>4</sub>, 1:3: mP8-FeB<sub>3</sub>, 1:2: oP12-FeB<sub>2</sub>.

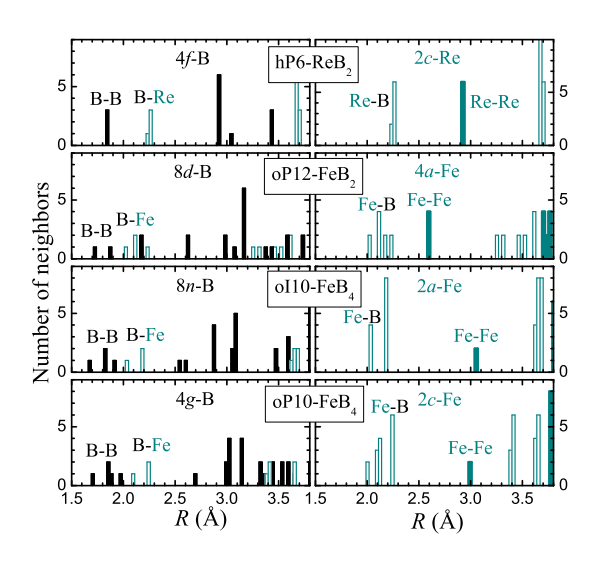


FIG. 3: (Color online) Nearest neighbor histograms in fully relaxed boron-rich Re-B and Fe-B structures. In oP10-FeB<sub>4</sub> the neighbors are shown only for one of the two 4g boron sites.

Comparison to published data. We use available information on stable iron and rhenium borides at ambient pressure to benchmark the performance of the generalized gradient approximation<sup>3</sup> employed in this study. For tI12-Fe<sub>2</sub>B and oP8-FeB our calculated magnetic moments, 1.85 and 1.16  $\mu_B/\text{Fe}$ , are in good agreement with previously measured values of 1.91 and 1.03  $\mu_B/\text{Fe}$ , respectively.<sup>4</sup> As shown in Table I, for tI12-Fe<sub>2</sub>B the calculated heats of formation are close to the previously calculated values but are noticeably larger in magnitude compared to the measured ones; for oP8-FeB we observe

		$\Delta H$ (kJ/mol of atoms)	Ref.
$tI12$ - $Fe_2B$	exp.	$-22.30^{a)}$	5
	exp.	$-22.60^{b)}$	5
	exp.	-23.71	6
	exp.	-(9.48-22.62)	7
	theo.	-32.09	6
	theo.	$-29.67^{c)}$	8
	theo.	$-30.30^{c)}$	This work
oP8-FeB	$\exp$ .	$-35.60^{a}$	5
	exp.	$-32.30^{b)}$	5
	theo.	$-35.48^{c)}$	8
	theo.	$-36.08^{c)}$	This work

TABLE I: Heat of formation for two stable compounds in the Fe-B system ( $^{a)}$  reference states:  $\alpha$ -Fe,  $\beta$ -B, T=298 K;  $^{b)}$  reference states:  $\gamma$ -Fe,  $\beta$ -B, T=1385 K;  $^{c)}$  values originally given in eV/atom).

an excellent agreement between theory and experiment. The elastic constants are determined by fitting the total energy of distorted unit cells to polynomials of second-order in strain. In order to determine all independent elastic constants for a given cell type, the same number of different strains is used. For each applied strain in the range [-0.03:0.03] with 0.01 steps the internal coordinates were fully relaxed. We find a generally good agreement between the present and previously reported values for the elastic constants and moduli, see Table II.

		$C_{11}$	$C_{12}$	$C_{13}$	$C_{22}$	$C_{23}$	$C_{33}$	$C_{44}$	$C_{55}$	$C_{66}$	B	G	E	$\nu$	Ref.
$tI12$ - $Fe_2B$	theo.	389.8	169.6	218.5			282.2	114.0		89.2	$249.7^{a)}$	$60.2^{a)}$	184.4	0.388	9
	theo.										$331.04^{b)}$	152.77	397.22	0.3	6
	theo.	413	154	132			389	148		157	228	143	355	0.24	This work
	exp.												343		10
	exp.												290		11,12
	exp.												300		13
	exp.										164				14
oP8-FeB	theo.	371	250	188	431	209	505	207	118	194	287	138	358	0.29	This work
	exp.												284		10
	$\exp$ .												350		11
	$\exp$ .												600		13
	exp.												125-624		15
											`	`			
$hP6-ReB_2$	theo.	641	159	128			1037	271			$350^{c)}$	$283^{c)}$			16
	theo.	631.3	158.4	133.8			1015.0	257.0			$347.7^{c)}$	$273.5^{c)}$			17
	theo.	689	170	141			1090	281			$369^{a}$	$294^{a)}$	696	0.19	18
	theo.	632	154	131			1005	248			$339^{a)}$	$266^{a)}$	632	0.19	This work
	exp.										360				19
	exp.										382	273			20
	exp.										371±22	302±18	712±43		21

TABLE II: Comparison of calculated elastic constants and moduli to previously reported theoretical and experimental values for selected known compounds. The elastic moduli were calculated using  $^{a)}$  Voigt-Reuss-Hill theorem,  $^{b)}$  equation of state, or  $^{c)}$  Voigt theorem.

- <sup>1</sup> G. Bergerhoff and I.D. Brown, in *Crystallographic Databases*, edited by F.H. Allen *et al.* (International Union of Crystallography, Chester,1987).
- <sup>2</sup> A.N. Kolmogorov, S. Shah, E.R. Margine, A.F. Bialon, T. Hammerschmidt, and R. Drautz, Phys. Rev. Lett. **105**, 217003 (2010).
- <sup>3</sup> J.P. Perdew, K. Burke, and M. Ernzerhof, Phys. Rev. Lett. 77, 3865 (1996).
- <sup>4</sup> R.S. Perkins, and P.J. Brown, J. Phys. F: Metal Phys. 4, 906 (1974).
- M. Palumbo, G. Cacciamani, E. Bosco, and M. Baricco, CALPHAD 25, 625 (2001) and references therein.
- <sup>6</sup> B. Xiao, J.D. Xing, J. Feng, C.T. Zhou, Y.F. Li, W. Su, X.J. Xie, and Y.H. Cheng, J. Phys. D: Appl. Phys. 42, 115415 (2009) and references therein.
- <sup>7</sup> S.P. Gordienko, Powder Metall. Met. Ceram. 41, 169 (2002) and references therein.
- <sup>8</sup> http://alloy.phys.cmu.edu/, accessed January 19th, 2010.
- <sup>9</sup> B. Xiao, J. Feng, C.T. Zhou, J.D. Xing, X.J. Xie, Y.H. Cheng, and R. Zhou, Physica B 405, 1274 (2010).
- <sup>10</sup> I. Ozbek, and C. Bindal, Surf. Coat. Technol. **154**, 14 (2002).
- <sup>11</sup> Y.A. Kunitskii, and É.V. Marek, Poroshkovaya Met. **99**, No. 3, 56 (1971).

- <sup>12</sup> D. Golanski, A. Marczuk, and T. Wierzchon, J. Mater Sci. Lett. **14**, 1499 (1995).
- <sup>13</sup> L.S. Lyakhovich, L.N. Kosachevskii, A.Y. Kulik, V.V. Surkov, and Y.V. Turov, Fiziko-Khimicheskaya Mekhanika Materialov, 99, No. 3, 34 (1973).
- <sup>14</sup> B. Chen, D. Penwell, J.H. Nguyen, and M.B. Kruger, Solid State Commun. **129**, 573 (2004).
- O. Culha, M. Toparli, S. Sahin, and T. Aksoy, J. Mater. Res. 206, 231 (2008).
- <sup>16</sup> W. Zhou, H. Wu, and T. Yildirim, Phys. Rev. B **76**, 184113 (2007).
- <sup>17</sup> R.F. Zhang, S. Veprek, and A.S. Argon, Appl. Phys. Lett. **91**, 201914 (2007) and references therein.
- <sup>18</sup> E. Zhao, J. Wang, J. Meng, and Z. Wu, J. Comput. Chem. 31, 1904 (2010).
- <sup>19</sup> H.Y. Chung, M.B. Weinberger, J.B. Levine, A. Kavner, J.M. Yang, S.H. Tolbert, and R.B. Kaner, Science 316, 436 (2007).
- <sup>20</sup> J.B. Levine, S.H. Tolbert, and R.B. Kaner, Adv. Funct. Mater. **19**, 3519 (2009).
- <sup>21</sup> H.Y. Chung, M.B. Weinberger, J.M. Yang, S.H. Tolbert, and R.B. Kaner, Appl. Phys. Lett. **92**, 261904 (2008).